Meccanica
https://doi.org/10.1007/s11012-019-01057-5


MECHANICS OF EXTREME MATERIALS

# Growth and remodeling in highly stressed solid tumors

**A. R. Carotenuto · A. Cutolo · S. Palumbo · M. Fraldi**

Received: 29 March 2019 / Accepted: 15 September 2019


**Abstract** Growing biological media develop residual stresses to make compatible elastic and inelastic growth-induced deformations, which in turn remodel the tissue properties modifying the actual elastic moduli and transforming an initially isotropic and homogeneous material into a spatially inhomogeneous and anisotropic one. This process is crucial in solid tumor growth mechanobiology, the residual stresses directly influencing tumor aggressiveness, nutrients walkway, necrosis and angiogenesis. With this in mind, we here analyze the problem of a hyperelastic sphere undergoing finite heterogeneous growth, in cases of different boundary conditions and spherical symmetry. By following an analytical approach, we obtain the explicit expression of the tangent elasticity tensor at any point of the material body as a function of the prescribed growth, by involving a *small-on-large* procedure and exploiting exact solutions for layered media. The results allowed to gain several new insights into how growth-guided mechanical stresses and remodeling processes can influence the solid tumor development. In particular, we highlight that—under hypotheses consistent with mechanical and physiological conditions—auxetic (negative Poisson ratio) transformations of the elastic response of selected growing mass districts could occur and contribute to explain some not yet completely understood phenomena associated to solid tumors. The general approach proposed in the present work could be also helpfully employed to conceive composite materials where ad hoc pre-stress distributions can be designed to obtain auxetic or other selected mechanical properties.

**Keywords** Tangent stiffness · Growth · Remodeling · Tumor · Auxetic

## 1 Introduction

Volumetric growth leads to adaptation processes that progressively transform the structure of a biological tissue through the co-evolution of stresses and mechanical properties, which arises in response to both mechanical stimuli and internal tissue activities resulting from physical as well as biochemical signals [8]. Mass accretion and structural remodeling, usually approached in literature through the use of finite deformations [9, 11, 24], can trigger processes of disparate nature that cooperate in order to drive tissue adaptation under mutable conditions. In this sense, soft tissues can be seen as complex composite

A. R. Carotenuto · A. Cutolo · S. Palumbo · M. Fraldi
Department of Structures for Engineering and Architecture, University of Napoli Federico II, Naples, Italy

M. Fraldi (✉)
Interdisciplinary Research Center for Biomaterials, University of Napoli Federico II, Naples, Italy
e-mail: fraldi@unina.it

Published online: 09 October 2019

materials in which living constituents are responsible for the temporal and spatial evolution of the material properties. Also, the interplay of growth, remodeling and repair processes occurring at the micro-scale, together with the associated mechanical stresses, becomes critical to discriminate the overall behavior and the functionality of the tissue [6]. Among these factors, the accumulation of growth-induced (residual) stress and the evaluation of the actual properties of the grown tissue are of particular interest from a biomechanical standpoint to fully characterize material remodeling. In fact, elastic deformation and residual stress—defined as the self-balanced stress field generating in a free traction body due to incompatible growth [37]—alter the initial tissue properties. On the other hand, abnormal stress levels can deviate the host tissue properties with respect to homeostatic conditions, by so compromising the microenvironmental physiology. This is the case of solid tumors, within which compressive stress seems to concur in many physiological events, such as the formation of hypoxic regions and vascular collapse [4, 44], directly involved in the nucleation of necrotic cores [21], peripheral migration and lymphangiogenesis associated to metastasis [27, 31, 42]. Stress gradients in biological media also rule nutrients supply, by driving the diffusion of chemicals within the fluid phase as well as macromolecules extravasation throughout the *interstitium*, in this way influencing cells proliferation, reconfiguration and motility. A vast literature has been dedicated to the investigation of tumor mechanical micro-environment to establish the nature of intratumoral residual stresses [2, 6, 37–39] and the related effects that they have on tumor progression. The mechanical characterization of these systems indeed represents a key aspect to envisage novel engineering-based strategies for reducing tumor aggressiveness, for example by enhancing intratumoral drug inflow, inhibiting peritumoral convective flow [18] or by selectively targeting tumor and healthy cells on the basis of their different mechanical properties at the single-cell scale level [14].

The presence of residual stress in grown tissues can be easily observed by means of experimental methods [7, 15]. However, ex vivo mechanical tests on excised tissue samples cannot reveal in what extent residual stress affects the intrinsic moduli. In this regard, the first part of the present work is aimed to individuate the way in which the resident growth-induced stress and growth-associated deformation determine the evolution of the elastic behavior of a growing body. In particular, the material remodeling of an initially isotropic mass has been investigated in terms of its tangent elastic properties, by revealing the onset of possible stress-induced inhomogeneity and anisotropy. The current expression of the elasticity tensor has been evaluated by exploiting a *small-on-large* approach [41], by tracing the mechanical response of a grown and stressed sample due to incremental superimposed deformations according to some literature formulations [5, 20, 25, 32]. These strategies have been adopted, for example, to characterize the kinematic hardening of elasto-plastic materials at finite strains [25] and also in biomechanical contexts [26] to study growth induced instabilities [19] or to investigate the fluid-structure interactions in hyperelastic blood vessels [3], in which the level of stress influences the structural integrity of the walls and supports the in vivo pressure regimes [28].

The growth-dependent moduli are here taken as a proxy to describe the alterations of the mechanical environment in spheroidal solid tumors, by discussing how they concur in tumor development. In addition, the variation of stress-induced heterogeneities in presence of high stress levels, typical of hyperproliferating tumors, has been analyzed in order to investigate possible unexpected material behaviors at advanced growth stages. In this regard, we have shown that growth—or, more in general, pre-stretch—can induce the formation of auxetic (Negative Poisson Ratio, NPR) phases, as a result of the interplay between nonlinear elastic deformation and energy storing in the form of residual stress. This counter-intuitive outcome is here specialized to the growth of solid tumor spheres to investigate the implications that the formation of a NPR coating can have on tumor progression, but it could be exploited for conceiving NPR bulky composites based on the design of the pre-stress in 3D-printed materials [47]. Therefore, in the second part of the work, we propose an analytical strategy according to which the remodeled body is treated as a sort of Functionally Graded Material (FGM), constituted by concentric hollow spheres with homogeneous stiffness. This strategy was already successfully applied to study spatially inhomogeneous composites for different engineering applications, e.g. for thermo-elastic analysis of FGM cylinders [12, 13]. By following this way, the overall mechanical

behavior of a growing remodeled body can be helpfully managed through the standard formalism and methods of linear elasticity.

## 2 Finite growth and remodeling of hyperelastic bodies

### 2.1 The effect of heterogeneous growth on residual stresses in spherical bodies

Growth is classically treated in the framework of finite elasticity as an independent inelastic contribution to the overall deformation of the body. According to this approach, the body mass elements grow by obeying their intrinsic biological programs that determine a variation of their volume and density, commonly accompanied by non-zero internal stress that elastically restores the compatibility of the grown tissue. The kinematics of a growing mass can be described by providing a multiplicative decomposition of the deformation gradient into the product of distinct aliquots, each of them mapping the body material points on a different configuration. More in detail, in an initially undeformed body $\mathscr{B}^t$ with volume $V^t$, usually denoted as reference configuration, the material points $\mathbf{X} \in \mathscr{B}^t$ are mapped at any time $t$ onto a current (spatial) configuration $\mathbf{x} \in \mathscr{B}^t$ by means of the one-to-one correspondence $\mathbf{x} = \chi(\mathbf{X}, t)$. Consequently, the motion of the body is completely governed by the total deformation gradient $\mathbf{F}$, which connects the differential position vectors of the two configurations, related to the displacement of the reference points $\mathbf{u}(\mathbf{X}, t) \in C^2(\mathscr{B}^t)$ through the compatibility equation:

$$\mathbf{F} = \frac{\partial \mathbf{x}(\mathbf{X}, t)}{\partial \mathbf{X}} = \mathbf{I} + \mathbf{u}(\mathbf{X}, t) \otimes \nabla_{\mathbf{X}} \tag{2.1}$$

where $\otimes$ and $\nabla_{\mathbf{X}}$ are respectively the dyadic product and the nabla vector with respect to material coordinates. In order to accomplish the presence of growth, the deformation gradient is assumed to be the multiplicative combination of a growth and an elastic term associated either to adaptation or to response to external loads [9, 33], i.e.

$$\mathbf{F} = \mathbf{F}_l \, \mathbf{F}_e \, \mathbf{F}_g \tag{2.2}$$

In absence of external loads, $\mathbf{F}_l = \mathbf{I}$ and the elastic and the growth parts of the deformation are the sole ones to eventually stress the body. Then, the body first undergoes traction-free growth that maps the reference body material points $\mathbf{X}$ on an intermediate configuration, say $\mathscr{B}^g$, in which they occupy the position $\mathbf{x}_g(\mathbf{X}, t) \in \mathscr{B}^g$. Non-homogeneous growth generally takes place in an incompatible manner [37], and elastic deformation is hence necessary to make compatible the independently grown elements, by exerting suitable self-equilibrated stresses. Therefore, the elastic strain $\mathbf{F}_e$ deforms the grown volume elements by mapping the points $\mathbf{x}_g \in \mathscr{B}^g$ onto the actual configuration $\mathbf{x} \in \mathscr{B}$, by accounting for the presence of growth-induced stresses (see Fig. 1).

In this work, the growth of a spherical body has been considered to model the development of spherical solid tumors, with the aim of studying how intratumoral stresses modify tissue properties, also leading to some nonstandard elastic behaviors. Solid tumors growth is the macroscopic result of unpredictable degenerating phenomena according to which malignant cells evade their natural program and undergo uncontrolled proliferation in one or more anatomic sites. These processes, that generally cannot be captured by means of a priori assigned growth curves, have been recently described by coupling the macroscopic growth kinematics with evolutionary competitive equations, capable of predicting the most relevant interactions occurring among healthy and tumor cell species that inhabit the tissue [6, 11]. The mechanobiology of tumor physiology has been largely investigated to provide an engineering-based interpretation of the most of biochemical and physical events underlying tumor formation and development. In particular, attention has been focused on the prediction of solid tumor growth and the characterization of growth-induced stresses and stress gradients, which actively influence some adverse mechanisms favoring tumor invasion and opposition to treatment [4, 38, 39]. For these reasons, the evaluation of intratumoral stresses as well as the prediction of the growth-induced remodeling of tumor tissue properties is diriment to envisage new mechanics-based strategies for attacking solid tumors. Considering the problem of a hyperelastic spherical solid tumor, a spherically symmetric geometry is introduced, so that $\mathbf{X} = \{R, \Theta, \Phi\}$ and the field variables depend only on

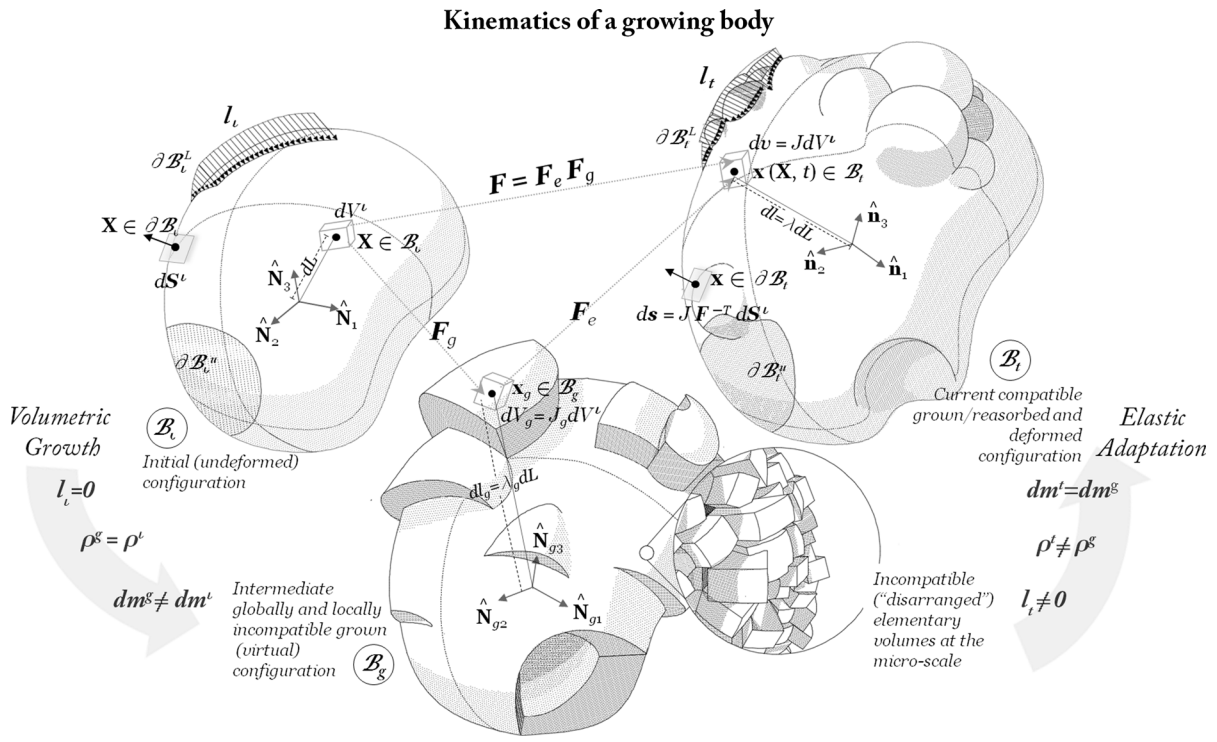


**Fig. 1** Hand-made sketch illustrating the kinematics of growth at finite strains obeying a multiplicative decomposition of the deformation gradient $\mathbf{F}$. This provides a growth part $\mathbf{F}_g$, which maps material points onto an intermediate and generally incompatible configuration, and an elastic part $\mathbf{F}_e$, which drives the body to the current compatible, grown and remodeled configuration

$R$. A spherical body is modeled by considering a thick spherical shell with an external radius $R_e$ and an inner radius $R_i \to 0^+$. Furthermore, spherical symmetry ensures that the deformation gradient $\mathbf{F}$ can be conveniently referred to its principal coordinates. By indicating with $\mathbf{x} = \{r, \theta, \phi\}$ the current coordinates, one has:

$$\mathbf{F} = \mathrm{Diag}\{\lambda_r \quad \lambda_\theta \quad \lambda_\phi\} = \mathrm{Diag}\left\{\frac{\partial r}{\partial R} \quad \frac{r}{R} \quad \frac{r}{R}\right\} \tag{2.3}$$

with $\lambda_\phi = \lambda_\theta$. The hypothesis of isotropic growth implies that $\mathbf{F}_g = \lambda_g \mathbf{I}$, $\lambda_g$ representing the growth stretch. Accordingly, also the elastic tensor $\mathbf{F}_e$ is diagonal:

$$\mathbf{F}_e = \mathbf{F}\,\mathbf{F}_g^{-1} = \mathrm{Diag}\left\{\frac{\lambda_r}{\lambda_g} \quad \frac{\lambda_\theta}{\lambda_g} \quad \frac{\lambda_\theta}{\lambda_g}\right\}, \qquad J_e = JJ_g^{-1} \tag{2.4}$$

where $J = \det\mathbf{F}$, $J_e = \det\mathbf{F}_e$ and $J_g = \det\mathbf{F}_g$ are the Jacobians of the transformations. In particular, $J_g = dV^g/dV^\iota = \lambda_g^3$ denotes the volume change due to growth, while $J_e$ measures elastic volumetric deformation in presence of a compressible tissue. Suitable constitutive assumptions are required to describe the tissue hyperelastic response and, in particular, a compressible version of the neo-Hookean strain energy density has been adopted [36, 45]:

$$\psi_e(\mathbf{F}_e) = \frac{\mu}{2}\left(J_e^{-2/3}\mathbf{F}_e : \mathbf{F}_e - 3\right) + \frac{\kappa}{2}(\log J_e)^2 \tag{2.5}$$

here $\mu$ and $\kappa$ are the initial material parameters representing the shear and the bulk modulus, respectively. They are related to the isotropic Young modulus $E$ and Poisson's ratio $\nu$ by means of the well-known relations $\mu = E/2(1+\nu)$ and $\kappa = E/3(1-2\nu)$. Standard thermodynamic considerations lead to the following expression for the Piola–Kirchhoff (nominal) and the Cauchy (actual) stress [28]:

$$\mathbf{P} = J_g \frac{\partial \psi_e}{\partial \mathbf{F}_e} \mathbf{F}_g^{-\mathsf{T}} \quad \text{and} \quad \sigma = J_e^{-1} \frac{\partial \psi_e}{\partial \mathbf{F}_e} \mathbf{F}_e^{\mathsf{T}} \tag{2.6}$$

that, with reference to the neo-Hookean potential (2.5), assume the form:

$$\begin{aligned} \mathbf{P} &= J_g \left[ \kappa (\log J_e) \mathbf{I} + \mu J_e^{-\frac{2}{3}} \left( \mathbf{b}_e - \frac{1}{3} (\mathbf{F}_e : \mathbf{F}_e) \right) \right] \mathbf{F}^{-\mathsf{T}} \\ &= J \sigma \mathbf{F}^{-\mathsf{T}} \end{aligned} \tag{2.7}$$

the two stress measures being connected through the Nanson's formula [10], while $\mathbf{b}_e = \mathbf{F}_e \mathbf{F}_e^{\mathsf{T}}$ is the left Cauchy–Green tensor. By supposing vanishing body forces and the velocity of growth to be much slower than that of the elastic wave in the body, the quasi-static balance of linear momentum is given by [10]:

$$\begin{aligned} &\nabla_{\mathbf{X}} \cdot \mathbf{P} = \mathbf{0}, \quad \forall \mathbf{X} \in \mathscr{B}^t \\ &\text{and} \\ &\nabla_{\mathbf{x}} \cdot \sigma = \mathbf{0}, \quad \forall \mathbf{x} \in \mathscr{B} \end{aligned} \tag{2.8}$$

The hypothesis of spherical symmetry implies the respect of the sole equilibrium equation along the radial direction:

$$\begin{aligned} &\frac{dP_{RR}}{dR} + \frac{2}{R} (P_{RR} - P_{\Phi\Phi}) = 0, \\ &\text{and} \\ &\frac{d\sigma_{rr}}{dr} + \frac{2}{r} (\sigma_{rr} - \sigma_{\phi\phi}) = 0 \end{aligned} \tag{2.9}$$

By focusing on the steady-state problem of a freely growing sphere, residual stresses are induced exclusively by heterogeneous growth [43]. For the sake of simplicity, a radially varying growth profile has been assigned, by means of the following parametric expression:

$$\lambda_g(R) = g_1 + (g_0 - g_1) \left( 1 - \left( \frac{R}{R_e} \right)^m \right) \tag{2.10}$$

The case $m = 2$ gives a parabolic trend already used in literature to reproduce the growth of spherical tumors [2], and returns a volumetric growth profile that qualitatively recalls the profiles of tumor fronts often recurring in tumor multiphase models [34], see Fig. 2. This trend also retraces progressive wave-like distributions of cancer volume fractions recently obtained via numerical simulations of tumor growth that provided a more elaborated coupling between poro-mechanical and multi-species competitive equations [6, 11]. As shown in Fig. 2, this profile identifies an inner bulk growth zone, where the space is almost entirely occupied by the hyper-proliferating tumor cells with maximum growth, and a transition zone in which, at a certain time $t$, there is only partial infiltration of the tumor, the growth pattern then decaying approaching the homeostatic host region. In Eq. (2.10), the values of the inner and peripheral growth stretch values, $g_0 > g_1$, need to be specified in accord with the aforementioned considerations. The corresponding elastic stretches and the stresses have been then computed by means of relations (2.4) and (2.6), respectively, and the integration of the equilibrium equation (2.9) has been performed numerically with the aid of the NDSolve package provided by the commercial software Mathematica®[46].

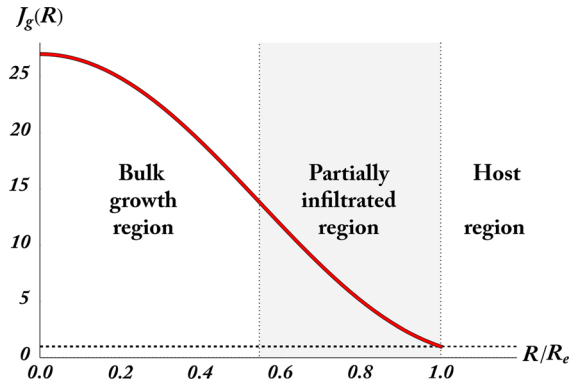


**Fig. 2** Qualitative behavior of the growth volume ratio, for $g_0 = 3$ and $g_1 = 1$

## 2.2 Growth-induced modification of tangent stiffness

Residual stresses and growth promote material remodeling processes that alter the initial isotropic behavior, by inducing a non-homogeneous and anisotropic elastic response. The tangent stiffness matrix of the grown sphere has been evaluated by using a *small-on-large* approach. This strategy provides that a small strain (the one related to the testing of the material properties starting from the current configuration) is superimposed to the (large) finite deformation experienced by the body and due to growth: this allows to express the updated moduli as explicit functions of the stress and of the stretch achieved after growth, in line the literature [3, 17, 26, 32, 41]. The motion applied to

the stressed body perturbs its current configuration by means of a deformation gradient $\mathbf{F}_s = \mathbf{I} + \mathbf{H}_s$, where $\mathbf{H}_s = \mathbf{u}_s \otimes \nabla_{\mathbf{x}}$ is the gradient of the additional displacement field $\mathbf{u}_s$ due to either traction or inelastic strains. The displacement gradient Ú of its symmetric and skew-symmetric parts, i.e. $\mathbf{H}_s = \mathbf{E}_s + \Omega_s$, respectively representing the infinitesimal strain and the rotation tensors under the assumption of small deformations. Therefore, the additional deformation multiplies the one related to the growth process, so that the new *small-on-large* deformation gradient reads as $\mathbf{F} = \mathbf{F}_s\mathbf{F}_0 = \mathbf{F}_s\mathbf{F}_{e0}\mathbf{F}_{g0}$, the subscript 0 being here used to denote the pre-stressed reference body on which tangent moduli are computed. Starting from the constitutive equations (2.6), and by also assuming that $J_s \simeq 1$, the updated Cauchy stress reads as:

$$\begin{aligned}\sigma &= J_0^{-1}\mathbf{F}_s\mathbf{F}_0\left(\mathbf{S}_0 + \frac{\partial \mathbf{S}}{\partial \mathbf{C}}\Big|_{\mathbf{C}_0} : (\mathbf{C} - \mathbf{C}_0)\right)\mathbf{F}_0^{\mathsf{T}}\mathbf{F}_s^{\mathsf{T}} \\ &= \mathbf{F}_s\left[\sigma_0 + 4J_{e0}^{-1}\mathbf{F}_0\left(\frac{\partial^2\psi_e}{\partial\mathbf{C}\partial\mathbf{C}}\Big|_{\mathbf{C}_0} : (\mathbf{F}_0^{\mathsf{T}}\mathbf{E}_s\mathbf{F}_0)\right)\mathbf{F}_0^{\mathsf{T}}\right]\mathbf{F}_s^{\mathsf{T}}\end{aligned} \tag{2.11}$$

where $\mathbf{S} = \mathbf{F}^{-1}\mathbf{P}$ is the second Piola–Kirchhoff stress and the relation $(\mathbf{C} - \mathbf{C}_0) = 2\mathbf{F}_0^{\mathsf{T}}\mathbf{E}_s\mathbf{F}_0$ has been used. Since $\mathbf{F}_s = \mathbf{I} + \mathbf{H}_s$, the hypothesis of small displacement gradient $\mathbf{H}_s$ leads to

$$\begin{aligned}\sigma \simeq\ & \sigma_0 + (\mathbf{I}\overline{\otimes}\,\sigma_0 + \sigma_0\underline{\otimes}\,\mathbf{I}) : \mathbf{H}_s \\ &+ \left[4J_{e0}^{-1}(\mathbf{F}_0\,\overline{\otimes}\,\mathbf{F}_0) : \frac{\partial^2\psi_e}{\partial\mathbf{C}\partial\mathbf{C}}\Big|_{\mathbf{C}_0} : (\mathbf{F}_0^{\mathsf{T}}\,\overline{\otimes}\,\mathbf{F}_0^{\mathsf{T}})\right] : \mathbf{E}_s\end{aligned} \tag{2.12}$$

Differentiation with respect to $\mathbf{E}_s$ gives the expression of the tangent stiffness

$$\begin{aligned}\mathbb{C} &= \frac{\partial\sigma}{\partial\mathbf{E}_s}\Big|_{\mathbf{F}_s\to\mathbf{I}} \\ &\simeq \frac{1}{2}(\mathbf{I}\,\overline{\otimes}\,\sigma_0 + \mathbf{I}\underline{\otimes}\,\sigma_0 + \sigma_0\,\overline{\otimes}\,\mathbf{I} + +\sigma_0\underline{\otimes}\,\mathbf{I}) \\ &\quad + 4J_{e0}^{-1}(\mathbf{F}_{e0}\,\overline{\otimes}\,\mathbf{F}_{e0}) : \frac{\partial^2\psi_e}{\partial\mathbf{C}_e\partial\mathbf{C}_e}\Big|_{\mathbf{C}_{e0}} : (\mathbf{F}_{e0}^{\mathsf{T}}\,\overline{\otimes}\,\mathbf{F}_{e0}^{\mathsf{T}}) \\ &\quad \simeq \mathscr{L}(\sigma_0) + \mathbb{E}_0\end{aligned} \tag{2.13}$$

that results to be a linear function of the residual stress, added up to a term that accounts for the the material stiffness tensor evaluated along the grown and stretched material fibers of the body, this structure somehow generalizing the well-known computation of the elastic modulus of a cord under constant tension. Also, in Eq. (2.13), the nonstandard tensor products $\overline{\otimes}$ and $\underline{\otimes}$ are respectively defined as $[\mathbf{A}\,\overline{\otimes}\,\mathbf{B}]_{ijkl} = A_{ik}B_{jl}$ and $[\mathbf{A}\,\underline{\otimes}\,\mathbf{B}]_{ijkl} = A_{il}B_{jk}$ [22, 23]. Then, this Kirchhoff-type stiffness can be re-organized in the more convenient Voigt $6\times 6$ notation, since *small-on-large* computation allows the preservation of major and minor symmetries of the tangent operator. By considering the neo-Hookean law (2.5), the term $\mathbb{E}_0$ in equation (2.13) results

$$\begin{aligned}\mathbb{E}_0 = \frac{2}{J_{e0}}\Bigg[&\kappa\left(\frac{1}{2}\mathbf{I}\otimes\mathbf{I} - (\log J_{e0})\mathbb{S}\right) + \\ &-\frac{\mu}{3}J_{e0}^{-\frac{2}{3}}(\mathbf{b}_{e0}\otimes\mathbf{I} + \mathbf{I}\otimes\mathbf{b}_{e0}) \\ &+\frac{\mu}{3}J_{e0}^{-\frac{2}{3}}(\mathbf{b}_{e0} : \mathbf{I})\left(\mathbb{S} + \frac{1}{3}\mathbf{I}\otimes\mathbf{I}\right)\Bigg]\end{aligned} \tag{2.14}$$

in which $\mathbb{S} = (\mathbf{I}\,\overline{\otimes}\,\mathbf{I} + \mathbf{I}\underline{\otimes}\,\mathbf{I})/2$ is the fourth-order identity tensor accounting for the symmetry of the deformation tensor $\mathbf{E}_s$ [22, 23]. Recalling constitutive equations (2.7), the equations (2.13) and (2.14) can be specialized to obtain the following independent tangent moduli:

$$\begin{aligned}C_{rrrr} &= \kappa J_{e0}^{-1} + \frac{4}{9}\mu J_{e0}^{-\frac{5}{3}}\left(2\lambda_{er0}^2 + \lambda_{e\phi 0}^2\right) \\ C_{rr\phi\phi} &= C_{rr\theta\theta} = \kappa J_{e0}^{-1} - \frac{2}{9}\mu J_{e0}^{-\frac{5}{3}}\left(2\lambda_{er0}^2 + \lambda_{e\phi 0}^2\right) \\ C_{\phi\phi\phi\phi} &= C_{\theta\theta\theta\theta} = \kappa J_{e0}^{-1} + \frac{2}{9}\mu J_{e0}^{-\frac{5}{3}}\left(\lambda_{er0}^2 + 5\lambda_{e\phi 0}^2\right) \\ C_{\theta\theta\phi\phi} &= \kappa J_{e0}^{-1} + \frac{2}{9}\mu J_{e0}^{-\frac{5}{3}}\left(\lambda_{er0}^2 - 4\lambda_{e\phi 0}^2\right) \\ C_{r\phi r\phi} &= C_{r\theta r\theta} = \mu J_{e0}^{-\frac{5}{3}}\left(\lambda_{er0}^2 + \lambda_{e\phi 0}^2\right)\end{aligned} \tag{2.15}$$

As shown by Eq. (2.15), with reference to the problem of a symmetric, initially isotropic sphere, the growth deformation and the associated residual stresses give back a tangent stiffness that exhibits transverse isotropy with respect to the radial direction, along which the remodeled moduli vary as explicit functions of the two elastic stretches. It can be easily shown that the matrix $\mathbb{C}$ is a positive-definite matrix for any $\lambda_{ei0} > 0$ under the assumption of small superimposed strain, and it reduces to the isotropic virgin elasticity tensor for vanishing elastic stretches. When the tissue

is finitely stretched by the growth, these functions instead allow to evaluate the local properties of the sphere and then to investigate its effective response under applied tractions. It is worth to highlight that the possibility of measuring such properties could be utilized, at least in principle, to gain information about the level of residual stress harbored within the mass, generally revealed by means of indirect and invasive techniques [6, 39]. For instance, information about these local properties (and consequently about the stresses) could be obtained from elastographic analyses, since Eq. (2.15) have a strict connection to the local density of the tissue. In fact, mass conservation principle under pure volumetric growth implies that $\varrho^t = \rho\, J_e$, $\varrho^t$ and $\rho$ being respectively the initial and the current densities, which are related to the elastic moduli in Eq. (2.15) through the tissue bulk response:

$$\kappa_0 = \frac{1}{9}\mathbf{I} : \mathbb{C} : \mathbf{I} = \frac{\kappa}{J_{e0}} = \frac{\kappa\,\rho_0}{\varrho^t} \tag{2.16}$$

Furthermore, by computing the compliance matrix $\mathbb{D} = [\mathbb{C}]^{-1}$, the two Poisson's Ratios (PRs) can be respectively given by $\nu_{r\phi} = -D_{12}/D_{11}$ and $\nu_{r\phi} = -D_{23}/D_{33}$, where $D_{ij} = [\mathbb{D}]_{ij}$, with expression

$$\nu_{r\phi} = \frac{3J_{e0}^{2/3}(1+\nu) - (1-2\nu)(2\lambda_{er0}^2 + \lambda_{e\phi 0}^2)}{6J_{e0}^{2/3}(1+\nu) + (1-2\nu)(2\lambda_{er0}^2 + \lambda_{e\phi 0}^2)} \tag{2.17}$$

$$\nu_{\phi\theta} = \frac{3\lambda_{er0}^3(1+\nu) - (1-2\nu)J_{e0}^{1/3}(2\lambda_{er0}^2 + \lambda_{e\phi 0}^2)}{3(1+\nu)(\lambda_{er0}^3 + J_{e0}) + (1-2\nu)J_{e0}^{1/3}(2\lambda_{er0}^2 + \lambda_{e\phi 0}^2)} \tag{2.18}$$

while the Young moduli are given by $E_r = D_{11}^{-1}$ and $E_\phi = D_{22}^{-1}$. In order to investigate the structural response of the heterogeneous remodeled sphere and to gain information about the effects of further incremental growth steps, an analytical strategy is proposed in what follows, based on the possibility of treating the grown body as a functionally-graded multilayer material (FGM), by considering a FG-sphere made of concentric and transversely isotropic layers with piece-wise constant moduli.

## 3 Characterization of the functionally graded grown sphere

At any fixed growth stage, the sphere exhibits the remodeled stiffness moduli given by the Eq. (2.15). In order to compute the *small* strain field and the updated Cauchy stress starting from the obtained radially varying stiffness matrix, the body is here treated as a functionally graded compound sphere, in which each layer exhibits transverse isotropy, the normal to the plane of isotropy being coaxial with the radial direction. By thus partitioning the domain into a sufficiently large number of layers, the FG-sphere can well approximate the continuous heterogeneous sphere. This strategy of solution allows to reduce the differential problem of the radially inhomogeneous sphere to an algebraic one of a $n$-layer transversely isotropic sphere. In particular, the assumed spherical symmetry allows to consider a unique displacement $u_r^{(i)}(r)$ in the generic $i$-th layer, this producing the following nonzero components of the strain $\mathbf{E}_s$:

$$\begin{aligned} \epsilon_{rr}^{(i)} &= \frac{d\,u_r^{(i)}(r)}{dr} - \omega_r^{(i)}\epsilon_a(r), \\ \epsilon_{\theta\theta}^{(i)} &= \epsilon_{\phi\phi}^{(i)} = r^{-1}u_r^{(i)}(r) - \omega_\phi^{(i)}\epsilon_a(r) \qquad i = 1, ..., n \end{aligned} \tag{3.1}$$

where $\epsilon_a(r)$ denotes an inelastic added strain field and $\omega_j^{(i)}$ are the anisotropy coefficients of the $i$-th layer. The layer-specific elastic constants $\overline{C}_{ijhk}^{(i)}$ can be obtained by averaging the varying moduli $C_{ijhk}(r) = [\mathbb{C}]_{ijhk}$ given by the Eq. (2.13) within each interval $r_i \le r \le r_{i+1}$:

$$\overline{C}_{ijhk}^{(i)} = \frac{1}{r_{i+1} - r_i}\int_{r_i}^{r_{i+1}} C_{ijhk}(\rho)\, d\rho, \tag{3.2}$$

The components of the stress $\sigma_s = \mathbb{C} : \mathbf{E}_s$ can be instead evaluated through the Hooke's generalized law, i.e.

$$\sigma_{rr}^{(i)} = \overline{C}_{rrrr}^{(i)}\,\epsilon_{rr}^{(i)} + 2\overline{C}_{rr\phi\phi}^{(i)}\epsilon_{\phi\phi}^{(i)}, \tag{3.3}$$

$$\sigma_{\phi\phi}^{(i)} = \sigma_{\theta\theta}^{(i)} = \overline{C}_{rr\phi\phi}^{(i)}\epsilon_{rr}^{(i)} + (\overline{C}_{\phi\phi\phi\phi}^{(i)} + \overline{C}_{\theta\theta\phi\phi}^{(i)})\epsilon_{\phi\phi}^{(i)} \tag{3.4}$$

the total stress $\sigma$ then reading as $\sigma \simeq \sigma_0 + \sigma_s$, in absence of rigid rotations because of spherical

symmetry. This hypothesis also allows to re-consider the sole radial equilibrium equation in each layer. Since the residual stress $\sigma_0$ is already self-equilibrated in force of the equation (2.9), equilibrium additionally requires that

$$\frac{d\sigma_{rr}^{(i)}}{dr}+\frac{2}{r}\left(\sigma_{rr}^{(i)}-\sigma_{\phi\phi}^{(i)}\right)=0 \tag{3.5}$$

Finally, by virtue of Eqs. (3.3), (3.2) and (3.1), the equilibrium can be written in terms of displacements as:

$$\frac{d^2u_r^{(i)}(r)}{dr^2}+\frac{2}{r}\frac{du_r^{(i)}(r)}{dr}-\alpha^{(i)}\frac{u_r^{(i)}(r)}{r^2}=\mathscr{E}_a(r) \tag{3.6}$$

representing a non-homogeneous Euler-like differential equation in which

$$\mathscr{E}_a(r)=\frac{1}{\overline{C}_{rrrr}^{(i)}}\left(k_r^{(i)}\frac{d\epsilon_a(r)}{dr}+2(k_r^{(i)}-k_\phi^{(i)})\epsilon_a(r)\right) \tag{3.7}$$

$$\alpha^{(i)}=2\frac{\overline{C}_{\phi\phi\phi\phi}^{(i)}+\overline{C}_{\theta\theta\phi\phi}^{(i)}-\overline{C}_{rr\phi\phi}^{(i)}}{\overline{C}_{rrrr}^{(i)}} \tag{3.8}$$

$$k_r^{(i)}=\omega_r^{(i)}\overline{C}_{rrrr}^{(i)}+2\,\omega_\phi^{(i)}\overline{C}_{rr\phi\phi}^{(i)} \tag{3.9}$$

$$k_\phi^{(i)}=\omega_r^{(i)}\overline{C}_{rr\phi\phi}^{(i)}+\omega_\phi^{(i)}(\overline{C}_{\phi\phi\phi\phi}^{(i)}+\overline{C}_{\theta\theta\phi\phi}^{(i)}) \tag{3.10}$$

are coefficients depending upon the elastic moduli of the $i$-th material. By denoting with

$$\beta^{(i)}=\left[\frac{1}{4}+2\frac{\overline{C}_{\phi\phi\phi\phi}^{(i)}+\overline{C}_{\theta\theta\phi\phi}^{(i)}-\overline{C}_{rr\phi\phi}^{(i)}}{\overline{C}_{rrrr}^{(i)}}\right]^{\frac{1}{2}} \tag{3.11}$$

the solution of Eq. (3.6) is

$$\begin{aligned}u_r^{(i)}(r)=r^{-1/2}\Big[&\left(A^{(i)}+\mathscr{I}_+^{(i)}(r)\right)r^{\beta^{(i)}}\\&+\left(B^{(i)}-\mathscr{I}_-^{(i)}(r)\right)r^{-\beta^{(i)}}\Big]\end{aligned} \tag{3.12}$$

Herein, $A^{(i)}$ and $B^{(i)}$ are integration constants while

$$\mathscr{I}_+^{(i)}(r)=\int_{r_i}^{r}\frac{1}{2\beta^{(i)}}\rho^{\frac{3}{2}-\beta^{(i)}}\,\mathscr{E}_a(\rho)d\rho \tag{3.13}$$

$$\mathscr{I}_-^{(i)}(r)=\int_{r_i}^{r}\frac{1}{2\beta^{(i)}}\rho^{\frac{3}{2}+\beta^{(i)}}\,\mathscr{E}_a(\rho)d\rho \tag{3.14}$$

let to find the particular solution of the problem. To obtain the unknowns $A^{(i)}$ and $B^{(i)}$, the conditions requiring the continuity of radial stresses and displacements at the interfaces are introduced:

$$\begin{cases}u_r^{(i-1)}\Big|_{r=r_i}=u_r^{(i)}\Big|_{r=r_i}\\ \sigma_{rr}^{(i-1)}\Big|_{r=r_i}=\sigma_{rr}^{(i)}\Big|_{r=r_i}\end{cases},\quad i=2,...,n \tag{3.15}$$

The boundary conditions instead provide null displacement on the vanishing internal inclusion $r_1\to 0$, while, on the outer surface, stress-prescribed or displacement-prescribed conditions can be alternatively considered by imposing either an external pressure $p$ or an assigned displacement $\delta_u$, i.e.:

$$\begin{cases}u_r^{(1)}\Big|_{r=r_1}=0\\ \sigma_{rr}^{(n)}\Big|_{r=r_{n+1}}=p\quad\text{or}\quad u_r^{(n)}\Big|_{r=r_{n+1}}=\delta_u\end{cases} \tag{3.16}$$

Then, by rearranging the $2n$ boundary conditions (3.15) and (3.16) by collecting the unknowns into a vector with structure $\mathbf{X}=\left[A^{(1)}\,B^{(1)}\,\cdots\,A^{(n)}\,B^{(n)}\right]_{2n\times1}^T$, a linear system of equations can be written down as

$$\mathbb{M}_\gamma\cdot\mathbf{X}=\mathbf{L}_\gamma+\mathbf{L}_a \tag{3.17}$$

where the subscript $\gamma=\{p,\delta\}$ discriminates between the traction- and displacement-prescribed problems, i.e. $\mathbf{L}_p=[0\;0\;\cdots\;0\;p]_{2n\times1}^T$ is the external loads vector, $\mathbf{L}_\delta=[0\;0\;\cdots\;0\;\delta_u]_{2n\times1}^T$ is the applied displacements vector, while $\mathbb{M}_p$ and $\mathbb{M}_\delta$ are the related $2n\times2n$ coefficient matrices, containing the sole geometric and constitutive information about the layers. Furthermore, $\mathbf{L}_a$ represents a vector containing all the terms deriving from the assigned inelastic strain. With the aim of discussing numerical strategies for inverting the matrix $\mathbb{M}_\gamma$, it is worth to notice the possibility of obtaining computational advantages by partitioning $\mathbb{M}_\gamma$ by means of a block tridiagonal matrix procedure, e.g. by realizing a special block matrix having square matrices (blocks) in the lower, main and upper diagonal, being all other blocks zero matrices. In this way, more efficient solution algorithms, such as

LU factorization or Thomas method, can be applied to compute the solution:

$$\mathbf{X} = \mathbb{M}_{\gamma}^{-1} \cdot \left(\mathbf{L}_{\gamma} + \mathbf{L}_{a}\right), \quad \gamma = \{p, \delta\} \tag{3.18}$$

With the help of this procedure, we analytically studied the effects that incipient growth produces on the heterogeneous remodeled sphere under different conditions. In particular, by identifying the inelastic strain with an incremental growth contribution and by preserving the hypothesis of isotropic growth, linearization of $\lambda_g = J_g^{1/3}$ implies

$$\begin{aligned} &\omega_r^{(i)} = \omega_\phi^{(i)} = \omega = \frac{1}{3} \quad \forall i = 1, \ldots, n \\ &\text{and} \\ &\epsilon_a(r) \simeq J_g^*(r) - 1 \end{aligned} \tag{3.19}$$

where $J_g^*(r) = (\lambda_g^*(r))^3$ is the additional growth stretch, which is assumed to have the same functional form of Eq. (2.10) and different growth parameters. Moreover, a straightforward evaluation of the effective properties in terms of bulk modulus can be given by means of standard homogenization methods. In fact, once obtained the constants of integration from equation (3.18) (for $\gamma = p$), an estimation of the overall bulk modulus for the multilayer FGM tumor sphere can be determined through the relation [29]:

$$\overline{\kappa} = \frac{p}{3\, u_r^{(n)}(r_{n+1})\, r_{n+1}^{-1}} \tag{3.20}$$

## 4 Results and discussion

### 4.1 Growth-induced stresses and implications on the growth potential

By first considering the growth of an hyperelastic unloaded sphere, numerical results have been obtained by integrating the equilibrium equation $(2.9)_1$, by imposing a traction-free external boundary and vanishing displacement at $R_i \to 0$. Once the growth stretch function (2.10) is prescribed, the resulting growth-associated Cauchy stresses can be analyzed with reference to Fig. 3a. The sphere is subjected to hydrostatic compression in the internal zone, the radial stress vanishing towards the periphery. On the contrary, the hoop stress passes from negative (compressive) to positive (tensile) values, which put in tension the external layers of the body. In this way, the outer layers deform to accommodate the internal thrust arising from the inner bulk growth. This stress distribution has different implications on tumor microenvironmental physiology. In fact, high intratumoral compression is directly involved into the collapse of blood and lymphatic vessels, this provoking undernourishment of inner tumor districts and their subsequent necrosis. Also, internal stresses constitute a mechanical hurdle that contrasts the inflow of substances and drives centrifugal fluid diversion, a fact that contemporary impedes drugs infiltration and promotes tumor progression, by delivering nutrients at the tumor front. In the outermost zone, occupied by the host-tumor region, the layers stretch circumferentially to follow the severe development of the internal core. The positive tension also induces a local increase of the areal perfusion, which further enhances the growth potential of the cells that migrate towards less compressed and more supplied sectors. In fact, the Darcy-type flux $\mathbf{q}$, governing the transport of macromolecules in a certain district of the sphere, can be considered proportional to the local surface deformation, which directly affects the pore permeability, and to the gradient of the hydrostatic stress $\sigma_{hyd0} = tr(\sigma_0)/3$, according to the relation $\eta^{-1}\mathbf{q} \propto J^{-1}\mathbf{F}\nabla_{\mathbf{X}}(\sigma_{hyd0})$, $\eta$ representing a reference hydraulic conductivity. As shown in Fig. 3b, there is an actual correspondence between the flux variable and the distribution of specific surface growth, which can be taken in the form $dS^g \simeq dV^g/dR^g \propto J_g R^2$. The two functions achieve their maximum in the region of coexistence of tumor and host, not yet completely invaded by the growing tumor phase, showing how the spherical cell layers are more prone to expand in presence of available nutrients and favorable stress conditions, e.g. lower hydrostatic compressions. For all these reasons, a deeper investigation of the actual mechanical behavior of such systems in terms of growth-induced material remodeling and mechanical characterization of the tumor proliferating parenchyma—that determines the outward tumor progression—could be helpfully exploited to build up new mechanics-based strategies apt to selectively attack the tumor masses.

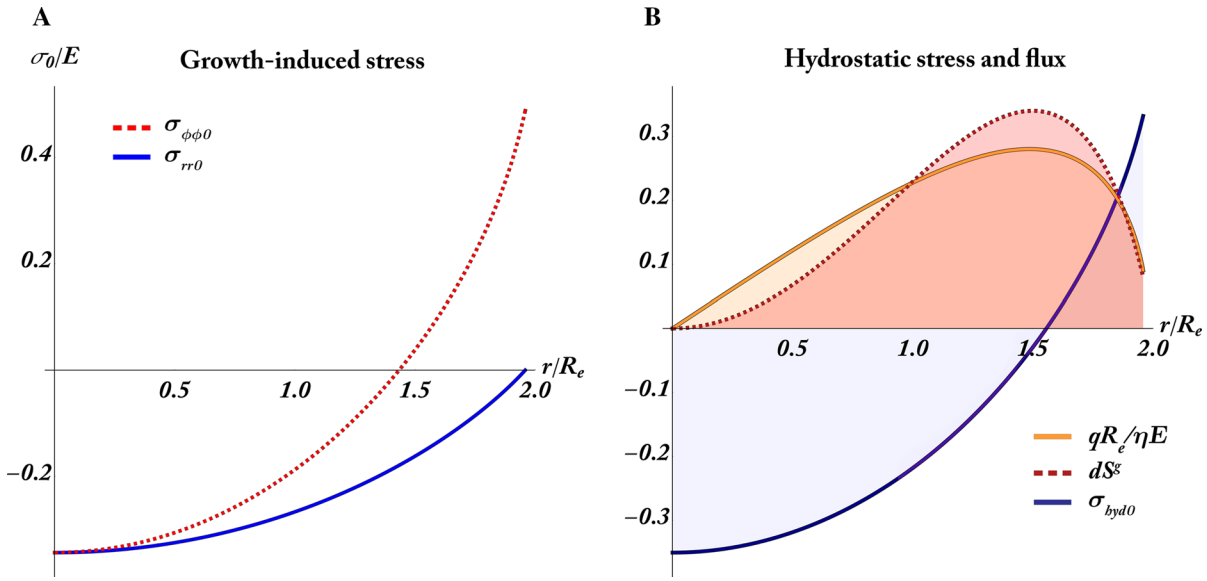


**Fig. 3** **a** Cauchy stresses in the grown and deformed sphere. **b** Relation between hydrostatic stress, normalized Darcy flow and variation of surface growth. The plot shows how increased pressure gradients drive nutrient walkways in the periphery of the tumor, by promoting the growth of external cell layers

### 4.2 Remodeled moduli, growth-induced stiffening and unusual findings

Once the stresses and the stretches due to growth are obtained, relations (2.15) were applied to determine the remodeled tangent properties of the sphere. Because of the spherical symmetry of the problem, the shear modulus $(2.15)_5$ was not taken into account. Figure 4a reports the trend of tangent moduli $C_{ijhk}$, given by Eq. $(2.15)_{1-4}$ and normalized with respect to the corresponding reference isotropic elasticity constants $C^l_{ijhk} = \mu\,(\delta_{ih}\delta_{jk} + \delta_{ik}\,\delta_{jh}) + (\kappa - 2\mu/3)\delta_{ij}\,\delta_{hk}$, as a function of the current radius $r$, normalized with respect to the initial sphere radius $R_e$. All the remodeled moduli exhibit a growth-induced stiffening in correspondence of the internal region interested by the bulk tumor growth, while, in the outermost transition region, the remodeled tissue softens since the elastic stiffness decreases if comparison with the corresponding initial moduli. A similar behavior is also exhibited by the radial and circumferential Young moduli in Fig. 4b, obtained from the compliance matrix. This is in accord with experimental findings showing that solid tumors are stiffer than their surrounding host [6, 38, 40, 45]. It could be inferred that this effect is used by tumor as a strategy for boosting its own development, since a stiffness gradient can actually work as a mechanical signaling pathway which may increase the migration potential of cancer cells. In fact, it has been experimentally observed that some cancer cells lineages, which mostly proliferate in the form of solid tumor spheroids in soft tissues, prefer softer environments for directional invasion. This suggests that a higher compliance of the surrounding host tissue might promote the migration of tumor cells invasion out of their stiffer primary location [16]. This was indeed confirmed in case of some types of breast cancer cells (MBA-MB-231, BT549, MCF7), pancreatic cancer cells (mPanc96, HPSC) and lung cancer cells (H60, A549) [16, 35, 40], despite there are cell phenotypes that seem instead to exhibit an opposite behavior, by preferring substrates with higher rigidity to initiate invasion [1, 30]. As a matter of fact, we can establish that a positive feedback occurs between bulk growth and invasion, since the mass growth would seem to affect the tumor mechanobiology by *per se* creating the conditions for activating mechanotaxis, by modifying the properties of the environment in which it is expanding.

Significant implications can be also derived from the analysis of the remodeled Poisson ratios, presented in Sect. 2.2. Figure 5a shows the trend of the PRs $\nu_{r\phi}$ and $\nu_{\phi\theta}$ (given by the Eq. (2.17)) for prescribed

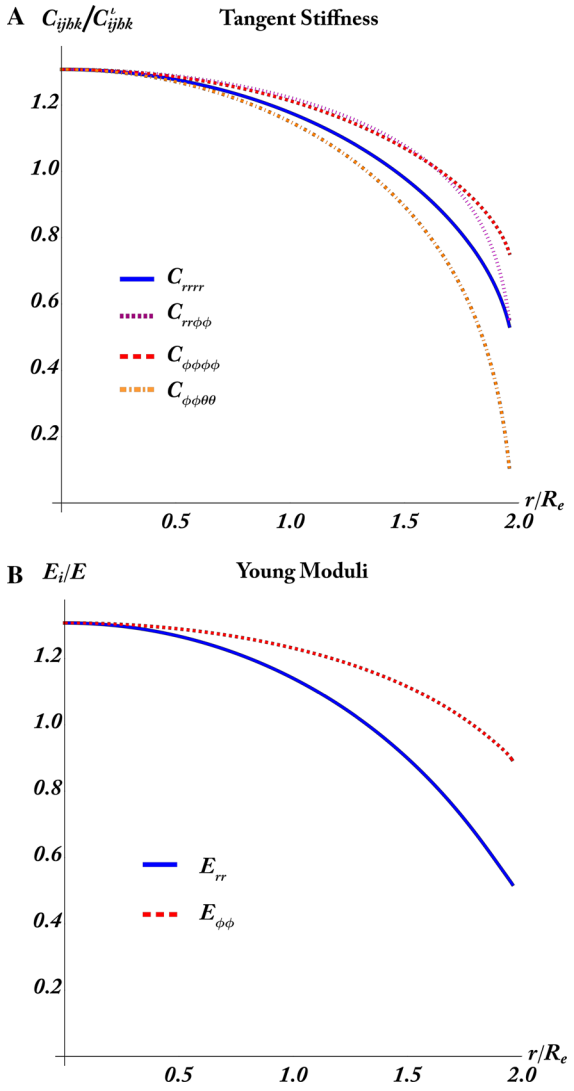


**Fig. 4** **a** Remodeled tangent stiffness constants in the heterogeneous sphere, **b** development of the corresponding radial and circumferential Young moduli. Tangent moduli are normalized with respect to the initial isotropic moduli, while, in the horizontal axis, the coordinate $r$ is normalized with respect to the reference tumor radius $R_e$

internal growth and mechanical parameters (i.e. $g_0 = 3$, $g_1 = 1$ and $\nu = 1/3$). More specifically, while the PR $\nu_{r\phi}$ weakly varies with respect to the reference PR, the Poisson coefficient $\nu_{\phi\theta}$ in the isotropy plane exhibits a more counter-intuitive and unseen behavior. In fact, by starting from the initial value at the tumor center, where a good degree of isotropy occurs, this PR decreases as it approaches the tumor periphery, by determining the conditions to have an auxetic behavior within a sort of coating placed at the outermost strata. The stretch-dependent formation of auxetic phases is analyzed more in detail in Fig. 5b, illustrating the behavior of the two tangent PRs, from Eq. (2.17), as a function of the ratio $\lambda_{er0}/\lambda_{e\phi 0}$. Herein, the tranversely isotropic PRs tend to the initial one under purely volumetric deformation, i.e. $\nu_{ij} = \nu$ when $\lambda_{er0} = \lambda_{e\phi 0}$, this happening at the tumor center as well, where cells experience hydrostatic compression. However, if the stretches ratio differs from one, the PRs can assume negative values as a function of the initial Poisson coefficient and the achieved deformation level. For example, in the case of a compressible solid tumor, the outer layers present a high circumferential dilation and radial contraction, this leading the PR $\nu_{\phi\theta}$ to belong to the auxetic region highlighted in the left side of Fig. 5b. The unexpected formation of a NPR coating could have a high inference in the mechanical characterization of tumor micro-environment and in the study of tumor physiology. A more compliant external phase with NPR could in fact accommodate the internal expansion of the sphere and therein increase surface permeability since, cooperating with both resident tensile hoop stresses and dilating stretches, it could contribute to enlarge micropores, vessel capillary cross sections and interstitial spaces, by so advantaging migrotion of cancer cells. Independently from this effect, which is in literature mostly associated to the action of tensile stress peaks occurring at the tumor-host interface [18, 38], the NPR region could have further influences on tumor progression. The development of an auxetic interface might represent a mechanical strategy for tumors to prolong the survival. As the spherical mass progressively expands, resources in fact lack in the tumor interior and the stress-induced hypoxia contributes to create apoptotic regions and eventual necrotic cores [6, 21]. Therefore, at advanced growth stages, the peritumoral vascularization and lymphangiogenesis become fundamental processes to further promote the proliferation of cells that reside on the peripheral tumor rings. In this particular situation, the local tissue properties can have a key role because, as shown in Fig. 5c, the growth-induced formation of an auxetic coating anticipates and induces a change-in-sign of the hydrostatic stress gradient and, consequently, of the associated flux at the external boundary. In this way, back-flow phenomena could be kindled at the

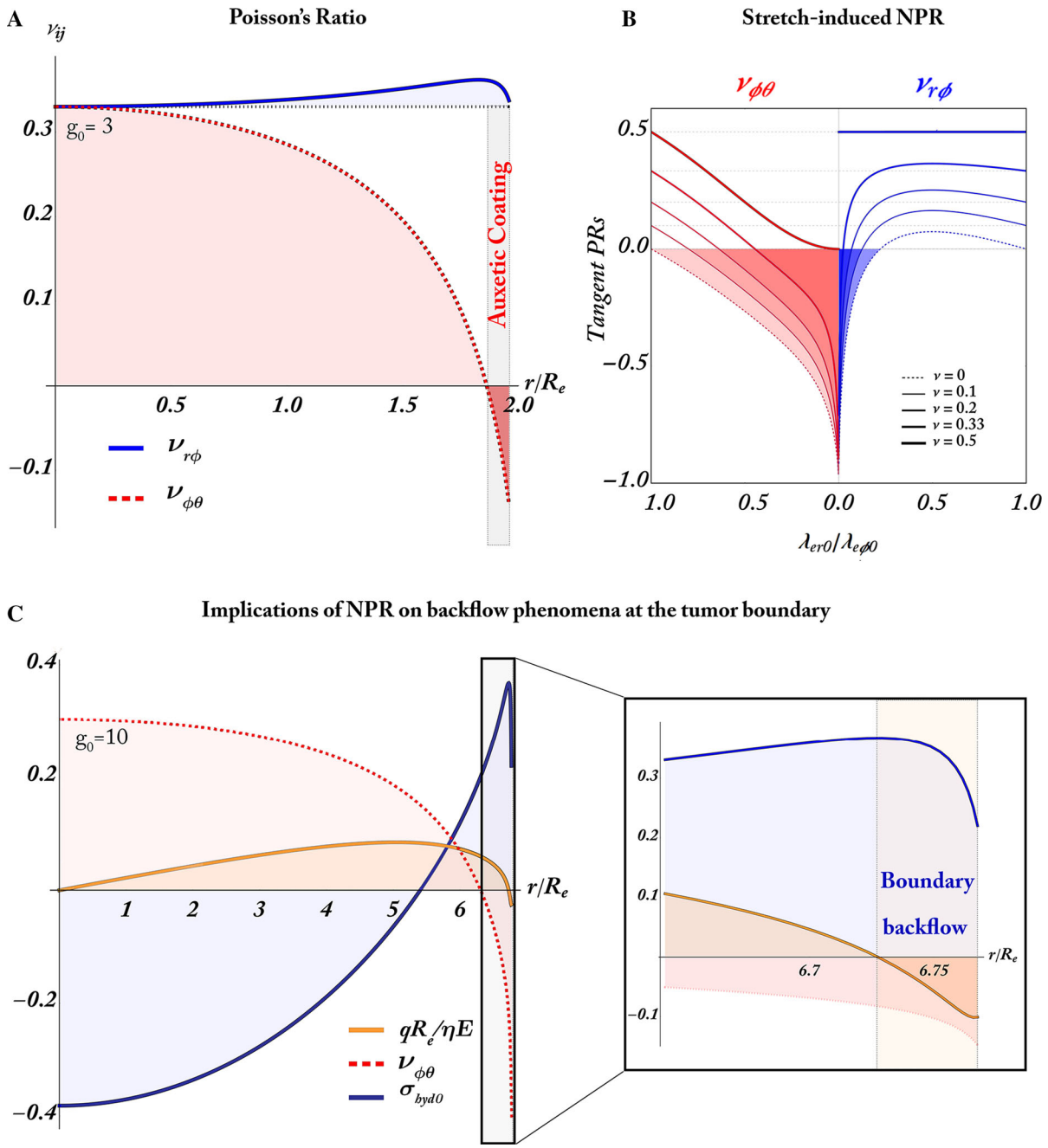


**Fig. 5** **a** Representation of the remodeled Poisson coefficients, with emphasis on the formation of the in-plane auxetic coating, **b** Tangent Poisson Ratios $\nu_{\theta\phi}$ (in red) and $\nu_{r\phi}$ (in blue) as a function of the ratio between the elastic stretches $\lambda_{er0}/\lambda_{e\phi 0}$ and of the initial PR $\nu$, providing the formation of NPR regions, **c** development of the auxetic coating at later growth stages and NPR-induced back-flow phenomena (in the inset). (Color figure online)

interface, thanks to which the severely grown mass can mechanically drive the intake of new resources from the exterior, also enhanced by the locally augmented permeability, so ensuring the survival of leading cancer cells through the penetration and the diffusion of metabolites. On the other hand, this outcome could be exploited, at least theoretically, to envisage new engineered infiltration strategies aimed to induce a

planned cyto-toxicity of the peripheral tumor environment in a way to increase the efficiency of chemicals delivery.

Apart the possible interest into tumor mechanobiology, it is worth to highlight that all the above considerations can be applied to more general situations. In fact, the outcomes demonstrated that the nonlinear deformation of a generic hyperelastic material and the elastic energy stored in the form of residual stress induced by inhomogeneous pre-stretch of any kind, lead to have—under some conditions—auxetic phases. In principle, materials with these properties could be artificially obtained by for instance building up functionally graded multilayer composites constituted of hollow spheres with *ad hoc* induced pre-stress, so designing the needed Poisson ratios on the basis of analytical approaches.

### 4.3 Additional growth and effective properties of the FGM sphere

The remodeled grown sphere with radially varying properties has been properly modeled as a functionally graded material, constituted of layers that exhibit a homogeneous and transversely isotropic stiffness matrix, which can be calculated from Eq. (3.2), according to the strategy discussed in Sect. 3. The deformed sphere has been partitioned in $n = 150$ layers with equal thicknesses, provided that sharp gradients of the variable stiffness constants and of the residual stress were avoided within each layer (in such a case, a denser subdivision is required). For the example at hand, Fig. 6 shows how the heterogeneous bulk modulus of the sphere is well approximated by the discrete variation of the bulk moduli of the FG structure, which also permits to analytically compute the homogenized bulk modulus by means of the Eq. (3.20) in presence of an external pressure $p$. If only the external pressure is applied, the spherical body will mostly respond obeying a Reuss-like system and, because of the illustrated external softening and under linear assumptions, it is expected that the actual average bulk modulus is smaller than the initial one (see Fig. 6).

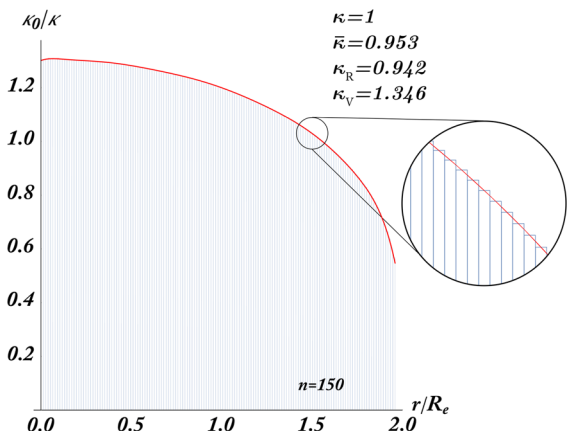


**Fig. 6** Evaluation of the composite bulk modulus in the FGM sphere. Data are normalized by the initial Young modulus $E$ ($g_0 = 3$, $g_1 = 1$, $\nu = 1/3$, $n = 150$ layers)

Then, additional growth deformation has been prescribed through Eq. (3.19), by assigning suitable incremental growth parameters (the values $g_0^* = 1.2$ and $g_1^* = 1.1$ have been adopted in the presented results). The two limit cases of unconfined growth and fully confined growth have been analyzed, respectively obtained by using $\sigma_{rr}^{(n)} = 0$ and $u_r^{(n)} = 0$ at $r = r_{n+1}$ as outer boundary conditions. The added heterogeneous growth profile induces an amplification of the internal stresses in a way that also depends on the inhomogeneous stiffness of the FGM. In particular, Fig. 7 shows how the pre-stress accumulated in the grown sphere (solid lines) modifies after the application of an incremental growth deformation. The stress components of the functionally graded sphere have been updated into each layer of the FGM both in unconfined and confined conditions, and then plotted together in order to return the overall stress profiles, by highlighting the established partition of the multilayer sphere. As shown in Fig. 7, in the displacement-prescribed case, the residual stress is affected by an almost entirely hydrostatic compression, determined as a reaction to the external confinement. On the other hand, in the unconfined condition, the stress amplification is more pronounced in the central region, where a higher growth deformation has been assigned and the remodeled layers result stiffer. In both the cases, heterogeneous properties can induce the accumulation of deviatoric stress (here represented in terms of von Mises stress in Fig. 7), which can potentially initiate yield phenomena by implying a further plastic-like tissue remodeling processes and cell re-organization, accompanied by a re-distribution of the stress within the spherical body.

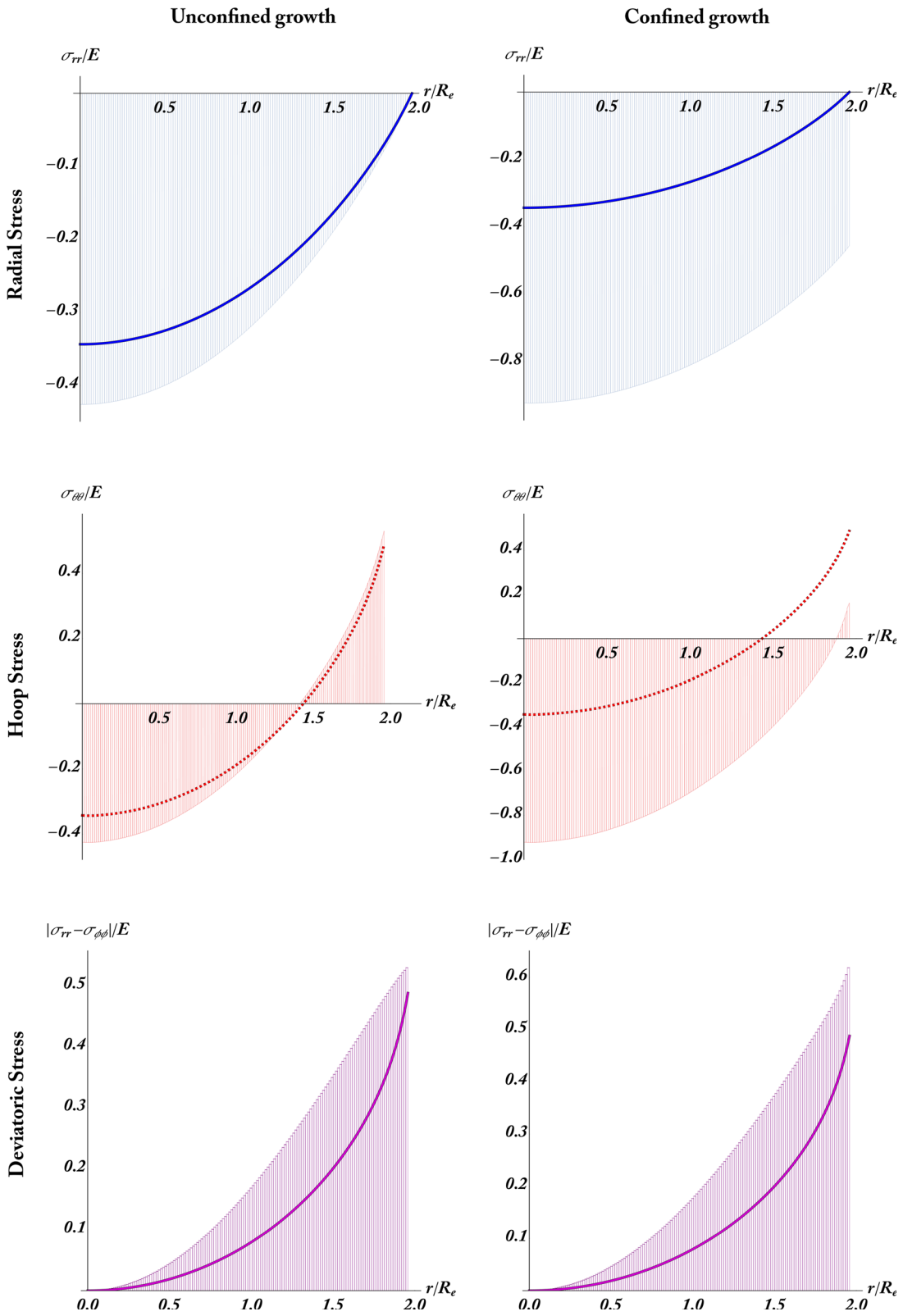
Unconfined growth
Confined growth
Radial Stress
Hoop Stress
Deviatoric Stress
$\sigma_{rr}/E$
$\sigma_{\theta\theta}/E$
$|\sigma_{rr}-\sigma_{\phi\phi}|/E$
$r/R_e$
0.5
1.0
1.5
2.0
0.0
−0.1
−0.2
−0.3
−0.4
−0.6
−0.8
−1.0
0.1
0.2
0.3
0.4
0.5
0.6

◀**Fig. 7** Radial stress (top), hoop stress (center) and von Mises stress (bottom). The solid lines represent the pre-stress components imprisoned in the grown sphere, then updated in each layer of the composite sphere after the application of an incremental growth deformation and plotted together in both the confined and unconfined cases ($g_0^* = 1.2$, $g_1^* = 1.1$ in both the simulations, $n = 150$ layers)

## 5 Conclusions

The nonlinear model here presented exploits the coupling between growth-induced stresses and deformation of a hyperelastic material to analyze the remodeling of a growing medium and study how tangent stiffness matrix accordingly changes. By approaching the problem in a fully general nonlinear framework, we obtained the explicit form of the tangent elastic moduli as functions of the growth profile and the associated residual stresses, demonstrating how, in case of spherical symmetry, the remodeling of the mechanical properties lead to a radially inhomogeneous and transversely isotropic material. Interestingly, we also found that, by setting some initial values compatible with mechanical and physiological conditions, outermost strata of the growing sphere can become auxetic, so exhibiting negative Poisson ratios whose magnitudes depend on the corresponding values they had in the reference stress-free configuration and on the actual strain level. In particular, we highlighted that the occurrence of this unseen growth-induced auxetic district in solid tumors parenchyma could have possible relevant implications on tumor development, by for example favoring backflow of nutrients and fluids at host-tumor interface which could be helpfully used to both better understanding solid tumor mechanobiology and planning drug delivery. Since the results were obtained by following analytical strategies, we also discussed the possibility of exploiting the method and the outcomes for envisaging new classes of composite materials with planned pre-stress designed to induce auxetic or other needed mechanical behaviors.

**Funding** This study was funded by the Italian Ministry of Education, Universities and Research through the Grants: "Integrated mechanobiology approaches for a precise medicine in cancer treatment" (Award Number: PRIN-20177TTP3S), "Micromechanics and robotics for diagnosis and therapy in prostate cancer" (Award Number: PON-ARS01_01384), "CIRO - Campania Imaging Infrastructure for Research in Oncology" (CUP B61G17000190007, SURF 17063BP000000002) and SATIN - "Therapeutic Strategies against Resistant Cancer" (CUP B61C17000070007, SURF 17061BP000000002).

**Compliance with ethical standards**

**Conflict of interest** The authors declare that they have no conflict of interest.

## References

1. Alexander NR, Branch KM, Parekh A, Clark ES, Iwueke IC, Guelcher SA, Weaver AM (2008) Extracellular matrix rigidity promotes invadopodia activity. Curr Biol 18(17):1295–1299
2. Araujo RP, McElwain DLS (2005) The nature of the stresses induced during tissue growth. Appl Math Lett 18(10):1081–1088. https://doi.org/10.1016/j.aml.2004.09.019
3. Baek S, Gleason R, Rajagopal K, Humphrey J (2007) Theory of small on large: potential utility in computations of fluid–solid interactions in arteries. Comput Methods Appl Mech Eng 196(31–32):3070–3078. https://doi.org/10.1016/j.cma.2006.06.018
4. Boucher Y, Jain RK (1992) Microvascular pressure is the principal driving force for interstitial hypertension in solid tumors: implications for vascular collapse. Cancer Res 52(18):5110–5114
5. Brannon R (1998) Caveats concerning conjugate stress and strain measures for frame indifferent anisotropic elasticity. Acta Mech 129(1–2):107–116
6. Carotenuto A, Cutolo A, Petrillo A, Fusco R, Arra C, Sansone M, Larobina D, Cardoso L, Fraldi M (2018) Growth and in vivo stresses traced through tumor mechanics enriched with predator-prey cells dynamics. J Mech Behav Biomed Mater. https://doi.org/10.1016/j.jmbbm.2018.06.011
7. Ciarletta P, Destrade M, Gower AL (2016) On residual stresses and homeostasis: an elastic theory of functional adaptation in living matter. Sci Rep 6(1), https://doi.org/10.1038/srep24390
8. Cowin SC (2006) On the modeling of growth and adaptation. In: Mechanics of biological tissue, Springer, pp 29–46, https://doi.org/10.1007/3-540-31184-x_3
9. Cowin SC (2010) Continuum kinematical modeling of mass increasing biological growth. Int J Eng Sci 48(11):1137–1145. https://doi.org/10.1016/j.ijengsci.2010.06.008
10. Cowin SC, Doty SB (2007) Tissue mechanics. Springer, Berlin
11. Fraldi M, Carotenuto AR (2018) Cells competition in tumor growth poroelasticity. J Mech Phys Solids 112:345–367
12. Fraldi M, Nunziante L, Carannante F (2007) Axis-symmetrical solutions forn-plies functionally graded material cylinders under strain no-decaying conditions. Mech Adv Mater Struct 14(3):151–174. https://doi.org/10.1080/15376490600719220
13. Fraldi M, Carannante F, Nunziante L (2013) Analytical solutions for n-phase functionally graded material cylinders under de saint venant load conditions: homogenization and

effects of poisson ratios on the overall stiffness. Compos Part B Eng 45(1):1310–1324. https://doi.org/10.1016/j.compositesb.2012.09.016
14. Fraldi M, Cugno A, Deseri L, Dayal K, Pugno NM (2015) A frequency-based hypothesis for mechanically targeting and selectively attacking cancer cells. J R Soc Interface 12(111):20150656. https://doi.org/10.1098/rsif.2015.0656
15. Fung Y (1981) Biomechanics: mechanical properties of living tissues. In: Fung YC (ed) Biomechanics. Springer, Berlin
16. Gu Z, Liu F, Tonkova EA, Lee SY, Tschumperlin DJ, Brenner MB (2014) Soft matrix is a natural stimulator for cellular invasiveness. Mol Biol Cell 25(4):457–469
17. Hoger A (1986) On the determination of residual stress in an elastic body. J Elast 16(3):303–324. https://doi.org/10.1007/bf00040818
18. Jain RK, Tong RT, Munn LL (2007) Effect of vascular normalization by antiangiogenic therapy on interstitial hypertension, peritumor edema, and lymphatic metastasis: Insights from a mathematical model. Cancer Res 67(6):2729–2735. https://doi.org/10.1158/0008-5472.CAN-06-4102
19. Javili A, Steinmann P, Kuhl E (2014) A novel strategy to identify the critical conditions for growth-induced instabilities. J Mech Behav Biomed Mater 29:20–32. https://doi.org/10.1016/j.jmbbm.2013.08.017
20. Ji W, Waas AM, Bazant ZP (2013) On the importance of work-conjugacy and objective stress rates in finite deformation incremental finite element analysis. J Appl Mech 80(4):041024
21. Katira P, Bonnecaze RT, Zaman MH (2013) Modeling the mechanics of cancer: effect of changes in cellular and extracellular mechanical properties. Front Oncol 3:145
22. Kintzel O (2006) Fourth-order tensors-tensor differentiation with applications to continuum mechanics. part ii: tensor analysis on manifolds. ZAMM 86(4):312–334. https://doi.org/10.1002/zamm.200410243
23. Kintzel O, Başar Y (2006) Fourth-order tensors–tensor differentiation with applications to continuum mechanics. part i: Classical tensor analysis. ZAMM 86(4):291–311. https://doi.org/10.1002/zamm.200410242
24. Kuhl E (2014) Growing matter: a review of growth in living systems. J Mech Behav Biomed Mater 29:529–543. https://doi.org/10.1016/j.jmbbm.2013.10.009
25. Lubarda V (1994) An analysis of large-strain damage elastoplasticity. Int J Solids Struct 31(21):2951–2964. https://doi.org/10.1016/0020-7683(94)90062-0
26. Lubarda VA, Hoger A (2002) On the mechanics of solids with a growing mass. Int J Solids Struct 39(18):4627–4664. https://doi.org/10.1016/S0020-7683(02)00352-9
27. Munson JM, Shieh AC (2014) Interstitial fluid flow in cancer: implications for disease progression and treatment. Cancer Manag Res 6:317
28. Nappi F, Carotenuto AR, Vito DD, Spadaccio C, Acar C, Fraldi M (2015) Stress-shielding, growth and remodeling of pulmonary artery reinforced with copolymer scaffold and transposed into aortic position. Biomechanics and Modeling in Mechanobiology. https://doi.org/10.1007/s10237-015-0749-y
29. Nemat-Nasser S, Hori M (2013) Micromechanics: overall properties of heterogeneous materials, vol 37. Elsevier, Amsterdam
30. Nguyen AV, Nyberg KD, Scott MB, Welsh AM, Nguyen AH, Wu N, Hohlbauch SV, Geisse NA, Gibb EA, Robertson AG et al (2016) Stiffness of pancreatic cancer cells is associated with increased invasive potential. Integr Biol 8(12):1232–1245
31. Paduch R (2016) The role of lymphangiogenesis and angiogenesis in tumor metastasis. Cellular Oncol 39(5):397–410
32. Piero GD (1979) Some properties of the set of fourth-order tensors, with application to elasticity. J Elast 9(3):245–261. https://doi.org/10.1007/bf00041097
33. Rodriguez EK, Hoger A, McCulloch AD (1994) Stress-dependent finite growth in soft elastic tissues. J Biomech 27(4):455–467. https://doi.org/10.1016/0021-9290(94)90021-3
34. Sciumé G, Shelton S, Gand Gray CT W, Miller Hussain F, Ferrari M, Decuzzi P, Schrefler BA (2013) A multiphase model for three-dimensional tumor growth. New J Phys 15: https://doi.org/10.1088/1367-2630/15/1/015005
35. Shukla V, Higuita-Castro N, Nana-Sinkam P, Ghadiali S (2016) Substrate stiffness modulates lung cancer cell migration but not epithelial to mesenchymal transition. J Biomed Mater Res Part A 104(5):1182–1193
36. Simo J, Taylor RL, Pister K (1985) Variational and projection methods for the volume constraint in finite deformation elasto-plasticity. Comput Methods Appl Mech Eng 51(1–3):177–208
37. Skalak R, Zargaryan S, Jain RK, Netti PA, Hoger A (1996) Compatibility and the genesis of residual stress by volumetric growth. J Math Biol 34(8):889–914. https://doi.org/10.1007/bf01834825
38. Stylianopoulos T, Martin JD, Chauhan VP, Jain SR, Diop-Frimpong B, Bardeesy N, Smith BL, Ferrone CR, Hornicek FJ, Boucher Y, Munn LL, Jain RK (2012) Causes, consequences, and remedies for growth-induced solid stress in murine and human tumors. Proc Natl Acad Sci 109(38):15101–15108. https://doi.org/10.1073/pnas.1213353109
39. Stylianopoulos T, Martin JD, Snuderl M, Mpekris F, Jain SR, Jain RK (2013) Coevolution of solid stress and interstitial fluid pressure in tumors during progression: implications for vascular collapse. Cancer Res 73(13):3833–3841. https://doi.org/10.1158/0008-5472.can-12-4521
40. Tilghman RW, Cowan CR, Mih JD, Koryakina Y, Gioeli D, Slack-Davis JK, Blackman BR, Tschumperlin DJ, Parsons JT (2010) Matrix rigidity regulates cancer cell growth and cellular phenotype. PLoS ONE 5(9):e12905. https://doi.org/10.1371/journal.pone.0012905
41. Truesdell C, Noll W (1965) The non-linear field theories of mechanics. In: The non-linear field theories of mechanics, Springer, Berlin, pp 1–541, https://doi.org/10.1007/978-3-642-46015-9_1
42. Tse JM, Cheng G, Tyrrell JA, Wilcox-Adelman SA, Boucher Y, Jain RK, Munn LL (2011) Mechanical compression drives cancer cells toward invasive phenotype. Proc Natl Acad Sci 109(3):911–916. https://doi.org/10.1073/pnas.1118910109
43. Vandiver R, Goriely A (2009) Differential growth and residual stress in cylindrical elastic structures. Philos Trans R Soc A Math Phys Eng Sci 367(1902):3607–3630. https://doi.org/10.1098/rsta.2009.0114
44. Vaupel P (2004) Tumor microenvironmental physiology and its implications for radiation oncology. Semin Radiat

Oncol 14(3):198–206. https://doi.org/10.1016/j.semradonc.2004.04.008
45. Voutouri C, Mpekris F, Papageorgis P, Odysseos AD, Stylianopoulos T (2014) Role of constitutive behavior and tumor-host mechanical interactions in the state of stress and growth of solid tumors. PLoS ONE 9(8):e104717. https://doi.org/10.1371/journal.pone.0104717
46. Wolfram Research I (2015) Mathematica. Wolfram Research, Inc, Champaign
47. Zurlo G, Truskinovsky L (2017) Printing non-euclidean solids. Phys Rev Lett 119(4):048001